1 **Uptake of Neisserial autotransporter lipoprotein (NalP) promotes an**

2 **increase in human brain microvascular endothelial cell metabolic activity**

3

4 **Osman A. Dufailu, Jafar Mahdavi, Dlawer A. A. Ala'Aldeen[1], Karl G. Wooldridge and**

5 **Neil J. Oldfield[*]**

6

7 School of Life Sciences, University of Nottingham, Nottingham, UK

8 [1]Present address: Middle East Research Institute, Dream City, Erbil, Kurdistan Region of Iraq

9

10 [*]For correspondence: Centre for Biomolecular Sciences, University of Nottingham,

11 University Park, Nottingham, NG7 2RD, UK. E: neil.oldfield@nottingham.ac.uk; T: (+44)

12 115 748 6122.

Abstract

Neisseria meningitidis is normally a human nasopharyngeal commensal but is also capable of causing life-threatening sepsis and meningitis. *N. meningitidis* secretes several virulence-associated proteins including Neisserial autotransporter lipoprotein (NalP), an immunogenic, type Va autotransporter harboring an S8-family serine endopeptidase domain. NalP has been previously characterized as a cell-surface maturation protease which processes other virulence-associated meningococcal surface proteins, and as a factor contributing to the survival of meningococci in human serum due to its ability to cleave complement factor C3. Here, recombinant NalP (rNalP) fragments were purified and used to investigate the interaction of NalP with host cells. Flow cytometry and confocal microscopy demonstrated binding and uptake of rNalP into different human cell types. High-resolution microscopy confirmed that internalized rNalP predominantly localized to the perinuclear region of cells. Abolition of rNalP protease activity using site-directed mutagenesis did not influence uptake or sub-cellular localization, but inactive rNalP (rNalP^{S426A}) was unable to induce an increase in human brain microvascular endothelial cell metabolic activity provoked by proteolytically-active rNalP. Our data suggests a more complex and multifaceted role for NalP in meningococcal pathogenesis than was previously understood which includes novel intra-host cell functions.

Highlights:

- Recombinant NalP is internalized by a variety of human cell types
- Internalized NalP is localized predominantly to the perinuclear region of cells
- Exposure to NalP provokes increases in cell metabolic activity
- Effects on cell metabolic activity are dependent on NalP proteolytic activity

40

41   **1. Introduction**

42   *Neisseria meningitidis* is an encapsulated Gram-negative diplococcus commonly

43   carried in the human nasopharynx. Carriers usually remain asymptomatic, but rarely

44   meningococci can reach the bloodstream which may lead to sepsis, and the cerebral-spinal

45   fluid (CSF) which can result in meningitis [1]. *N. meningitidis* elaborates numerous virulence

46   factors that facilitate colonization and virulence [2]. One important class, which are also

47   found in many other Gram-negative bacteria, are the autotransporter (or type V-secreted)

48   proteins [3]. These comprise an N-terminal signal peptide and C-terminal β-domain, which

49   facilitate export of a central functional passenger domain across the Gram-negative inner and

50   outer membranes, respectively. Following export, the passenger domain may be cleaved and

51   released, either auto-catalytically or via a second protease, cleaved but remain non-covalently

52   bound to the translocator domain, or remain uncleaved and displayed at the cell surface [4].

53   Autotransporter passenger domains undertake a range of virulence-associated functions

54   including proteolytic, cytotoxic or adhesive activities [5].

55   The functional passenger domain of Neisserial autotransporter lipoprotein (NalP), also

56   termed autotransporter serine protease A (AspA), harbors an S8-family peptidase (subtilisin)

57   domain [6, 7]. Additionally, NalP expression is phase-variable via slipped strand mispairing,

58   a process mediated by a poly-cytosine tract within the protein-coding sequence [7, 8]. Auto-

59   catalytic proteolytic cleavage results in the release of a *ca.* 68-70 kDa passenger domain into

60   the external environment [6, 7]. However, a proportion of the cleaved passenger domains

61   remain, at least temporarily, anchored on the cell surface by an N-terminal lipid moiety [9].

62   This delayed or partial release facilitates the NalP-dependent proteolytic release of fragments

of other meningococcal surface proteins including: IgA1 protease; MspA (meningococcal serine protease A); App (adhesion and penetration protein); LbpB (lactoferrin-binding protein); and NHBA (Neisserial heparin binding antigen) [7, 10-14]. The consequences of the NalP-mediated release of meningococcal surface protein fragments on pathogenesis are beginning to be elucidated. For example, NalP-mediated release of NHBA abrogates extracellular DNA-mediated biofilm formation [15]. Furthermore, the NHBA-derived C2 fragment released following cleavage by NalP alters endothelial integrity by producing reactive oxygen species resulting in the internalization of the VE-cadherin adherens junction protein [16].

In addition to meningococcal targets, NalP has also been shown to cleave the host serum protein complement 3 (C3) [17]. NalP-mediated cleavage generates a functionally inactive C3a-like molecule, with the corresponding C3b-like fragment being rapidly inactivated by host serum factors resulting in the inhibition of C3b deposition on the bacterial surface and enhanced meningococcal serum resistance [17]. We hypothesized that, in addition to previously identified roles, NalP, like several other meningococcal autotransporter proteases [18-20], may also interact with host cells. Here we show uptake of NalP into various human cell types, and an increase in human brain microvascular endothelial cell metabolic activity which is dependent on NalP proteolytic activity.

2. Materials and Methods

2.1. Bacterial strains and culture conditions

Escherichia coli strain JM109 (Promega) was used for expression of recombinant His$_6$-tagged NalP passenger domain fragments. *E. coli* strain XL10-Gold (Agilent Technologies) was used for mutagenic plasmid construction. Strains were cultured at 37°C in Lysogeny broth (LB) or on LB agar supplemented with ampicillin (100 µg ml^{-1}). *N.*

88 *meningitidis* strain MC58 (ATCC® BAA335™) was cultured at 37°C, in an atmosphere of

89 air plus 5% CO_2, on Columbia agar with chocolated horse blood (Oxoid).

90

91 *2.2. Construction of plasmids encoding recombinant NalP proteins*

92   Primers NalPF1 (CGC<u>GGATCC</u>CTGCATACCGGAGACTTTCC) and NalPR1

93 (CGC<u>GGATCC</u>GGCGAGACTGTTGAAGATGCG) were used to amplify a fragment of *ca.* 2 kb

94 encoding amino acids ^{101}L to ^{784}A from *N. meningitidis* MC58 *nalP*. After digestion with

95 BamHI, the PCR product was ligated into BamHI-digested pQE30 to yield plasmid pOD1. A

96 single-nucleotide mutation (T to G) at nucleotide position 1276 of *nalP* was introduced into

97 pOD1 using the QuikChange Lightning site-directed mutagenesis kit (Agilent Technologies)

98 for expression of rNalP^{S426A}. The mutagenic reaction was undertaken following the

99 manufacturer's instructions and utilized primers t1276g S426A

100 (CCGATTCAAATTGCCGGAACAGCCTTTTCCGCACC) and t1276g_antisense

101 (GGTGCGGAAAAGGCTGTTCCGGCAATTTGAATCGG) to yield pOD1^{S426A}.

102

103 *2.3. Protein expression and purification*

104   rNalP and rNalP^{S426A} were expressed in *E. coli* JM109 harboring pOD1, or

105 pOD1^{S426A}, respectively, and purified under non-denaturing conditions. Briefly, *E. coli*

106 JM109 strains were grown to OD_{600} 0.5 before being induced with 1 mM IPTG and incubated

107 at 37°C for 3 h. Cells were harvested by centrifugation (4,200 × *g* for 10 min) and

108 resuspended in 30 ml lysis buffer (50 mM Na_2PO_4, 300 mM NaCl and 20 mM imidazole, pH

109 7.4) followed by sonication using a MSE SoniPrep 150 sonicator for 8 cycles (30s on, 30s

110 off) on ice. The cell lysate was centrifuged at 4,200 × *g* for 15 min and the cleared lysate

111 loaded onto a 1 ml Nickel-charged HisTrap FF column connected to a ÄKTAprime plus

112 liquid chromatography system (GE Healthcare Lifesciences) equilibrated with 10 column

113   volumes of wash buffer (50 mM Na_2PO_4, 300 mM NaCl and 40 mM imidazole, pH 7.4).

114   Proteins were eluted by step elution with appropriate buffer (50 mM Na_2PO_4, 300 mM NaCl

115   and 300 mM imidazole, pH 7.4). A HiTrap column pre-packed with five milliliters of

116   Sephadex G-25 Superfine (GE Healthcare Lifesciences) equilibrated with 5 column volumes

117   of phosphate buffered saline (PBS) was used for buffer exchange. His_6-tagged recombinant

118   *E. coli* trigger factor protein (rTF), encoded by the plasmid pCold TF (Takara Bio), was

119   purified as previously described [18]. Protein concentration was measured using the Pierce

120   BCA protein assay kit (Thermo Fisher Scientific) following endotoxin removal using Pierce

121   High Capacity Endotoxin removal spin columns (Thermo Fisher Scientific).

122

123   *2.4. SDS-PAGE and immunoblot analysis*

124   Proteins electrophoretically separated using polyacrylamide mini gels (Mini-Protean

125   III; Bio-Rad) were stained with SimplyBlue™ SafeStain (Thermo Fisher Scientific) for 1 h.

126   Alternatively proteins were transferred to nitrocellulose membranes and probed with rabbit

127   polyclonal anti-NalP [6] or mouse anti-pentahistidine antibody (Qiagen) diluted 1:5,000 or

128   1:2,000, respectively, in blocking buffer (5% [w/v] non-fat dry milk, 0.1% [v/v] Tween 20 in

129    $1 \times$ PBS) and incubated for 2 h. Following washing in PBS with 0.1% Tween 20 (PBST),

130   membranes were incubated for 2 h with goat anti-rabbit (or anti-mouse) IgG-alkaline

131   phosphatase conjugate (Sigma) at a dilution of 1:30,000 in blocking solution. After washing

132   with PBST, blots were developed using BCIP/NBT-Blue liquid substrate (Sigma).

133

134   *2.5. Cell culture*

135   All cells were maintained at 37°C in a humidified atmosphere of 5% CO_2. Cell culture

136   reagents were purchased from ScienCell unless otherwise stated. Human brain microvascular

137   endothelial cells (HBMECs-ATCC) were cultured on human fibronectin-coated flasks (BD

138   Biosciences) in basal endothelial cell medium, supplemented with 5% (v/v) heat-inactivated

139   fetal bovine albumin (FBS), $1 \times$ endothelial cell growth supplement and 1% (v/v) antibiotic /

140   anti-mycotic solution. Dendritic cells were generated as previously [18], and subsequently

141   grown in RPMI (Sigma) supplemented with 10% FBS and 1% antibiotic / anti-mycotic.

142   Human brain (cerebral cortex) astrocytes (ScienCell) were cultured in astrocyte growth

143   medium supplemented with 5% FBS, $1 \times$ astrocyte growth supplement and 1% antibiotic /

144   anti-mycotic. Hep-2 cells were cultured in DMEM (Sigma) supplemented with 10% FBS, $1 \times$

145   non-essential amino acids (Sigma) and 1% antibiotic / anti-mycotic.

146

147   *2.6. Flow cytometry*

148   HBMECs were cultured on fibronectin-coated 24-well plates for 16 h from a seeding

149   density of 5×10^4 cells ml^{-1}. rNalP was atto488-labelled using the Lightning-Link

150   conjugation kit (Innova Biosciences) according to the manufacturer's instructions. Cells were

151   treated with atto488 alone, atto488-labelled rNalP or unlabeled rNalP (250 nM final

152   concentration dissolved in media) for 8 h. Cells were washed with PBS, fixed with 2%

153   paraformaldehyde for 10 min, and washed again with PBS before being detached using

154   trypsin-EDTA (Sigma). Harvested cells were washed twice with PBS and finally resuspended

155   in 500 µl of PBS. Samples were run on a FC500 flow cytometer (Beckman Coulter). 100,000

156   events were recorded, and acquired data was analyzed using Kaluza v1.3 software.

157

158   *2.7. Cell internalization assays*

159   Proteins were Cy5-labelled using the Lightning-Link conjugation kit (Innova

160   Biosciences) according to the manufacturer's instructions. Cells were seeded onto acid-

161   etched 12 mm glass coverslips (pre-coated with 0.1% human fibronectin for HBMECs) in 24-

162   well plates at a seeding density of 5×10^4 cells per well and incubated for 16 h. Cells were

163 treated with labelled rNalP or rTF (250 nM final concentration dissolved in media) for 45

164 min, 2 h, 4 h or 8 h. After treatment, cells were washed thrice with PBS, fixed in 4%

165 paraformaldehyde for 10 min, and rinsed thrice in PBS. Cells were mounted using proLong

166 Gold anti-fade with DAPI (Life Technologies) to stain cell nuclei. Confocal imaging was

167 performed using a Zeiss LSM 700 confocal laser-scanning microscope using a Plan-

168 Apochromat 63×/1.40 Oil DIC M27 objective with ZEN 2009 operating software, and

169 equipped with lasers at 633 and 405 nm for excitation of Cy5 and DAPI, respectively. The

170 images collected in the two channels were later merged and analyzed using Zeiss LSM and

171 ImageJ software. Structured illumination microscopy (SIM) images were captured on a Zeiss

172 Elyra PS.1 microscope using an Objective alpha Plan-Apochromat 100×/1.46 Oil DIC M27

173 objective with ZEN 2012 acquisition and processing software. Samples were excited using

174 the 642 and 405 nm laser lines and fluorescence was detected using the LP 655 filter set. 3D

175 reconstruction was carried out using ZEN 2012 Black software. 30,000 images were

176 processed where single molecule events were identified with the peak intensity to noise value

177 set to ten.

178

179 *2.8. Human Complement 3 (C3) protein cleavage assay*

180 This was performed as previously described [17] with minor modifications. Briefly,

181 40 nM recombinant protein was mixed with 250 ng human complement 3 (C3; Sigma) in

182 PBS and incubated at 37°C with shaking for 16 h. C3 cleavage was determined by

183 immunoblot analysis using goat anti-human C3 antibody (diluted 1:5000; Sigma) and rabbit

184 anti-goat IgG alkaline phosphatase conjugate (diluted 1:30000; Sigma).

185

2.9. XTT assay

HBMECs were seeded in 96-well plates (1×10^4 cells well^{-1}) and grown overnight as outlined in section 2.5. Cells were supplied with serum-free media and incubated at 37°C with 5% CO_2 for 1 h before the addition of recombinant protein (40 nM final concentration) and XTT detection solution (Cell Signaling Technologies). Cells were incubated for 37°C with 5% CO_2 for 750 min and absorbance measurements (450 nm) taken using a Spark microplate plate reader. Each test was performed in triplicate wells and on a least three independent occasions. GraphPad Prism v7 was used to analyze the data using two-way ANOVA and Tukey's multiple comparison test. A *p* value < 0.05 was considered statistically significant.

2.10. Histone clipping

Recombinant core histones (New England Biolabs; 200 μg ml^{-1} final concentration) and purified recombinant protein (40nM final concentration) were mixed in a total volume of 40 μl PBS, and incubated at 37°C for 16 h. Reactions were stopped by the addition of 5 × sample buffer (0.62 M Tris-HCl [pH 6.8], 5% SDS, 25% glycerol, 12.5% β-mercaptoethanol, 0.25 M DTT, 0.002% bromophenol blue), followed by immediate boiling for 5 min. Aliquots of cleavage products were subjected to SDS-PAGE, and gels strained with SimplyBlue™ SafeStain (Thermo Fisher Scientific).

3. Results

3.1. NalP is internalized by human cells

The passenger domain of the group B meningococcal strain MC58 NalP protein was expressed in *E. coli* and purified under non-denaturing conditions to yield rNalP. Co-incubation with human brain microvascular endothelial cells (HBMECs) followed by

211   examination by flow cytometry showing a clear shift in fluorescence signal in HBMECs

212   treated with fluorescently labelled rNalP compared with HBMECs treated with label alone or

213   with unlabeled rNalP, suggesting the direct interaction of rNalP with host cells (Fig. 1).

214   Confocal laser scanning microscopy was subsequently used to visualize rNalP following co-

215   incubation with HBMECs (Fig. 2). From 2 h co-incubation, internalized rNalP was primarily

216   apparent in crescent-like perinuclear accumulations (Fig. 2). In contrast, an unrelated His_6-

217   tagged recombinant protein (*E. coli* trigger factor; rTF), which was purified using the same

218   methodology as rNalP, was not internalized, demonstrating cellular specificity for rNalP

219   uptake (Fig. 2). Localization of internalized rNalP predominantly to the perinuclear region of

220   HBMECs was confirmed using high-resolution microscopy (Fig. S1). Examination by

221   confocal microscopy of other human cell types, including dendritic cells (DCs), epithelial

222   cells (Hep-2) and neural cells (astrocytes) showed that rNalP was also taken up by these cell

223   types and similarly localized to the cytoplasmic and/or perinuclear regions (Fig. S2).

224

225   *3.2. Uptake of proteolytically-active rNalP promotes an increase in HBMEC metabolic*

226   *activity*

227   Site-directed mutagenesis was used to replace the catalytic serine residue of rNalP

228   with alanine to generate rNalP^{S426A}. The abolition of proteolytic activity was confirmed by

229   the inability of rNalP^{S426A} to generate a *ca.* 100-kDa α-chain fragment following incubation

230   with the NalP target human complement factor C3 [17] (Fig. S3). Examination by confocal

231   microscopy showed no apparent differences in the localization of rNalP^{S426A} or rNalP in

232   HBMECs after co-incubation of cells with these proteins, showing that rNalP proteolytic

233   activity was not required for uptake or subsequent sub-cellular localization (Fig. 3).

234   To examine the cellular response to NalP, HBMECs were monitored post-exposure to

235   rNalP or rNalP^{S426A} using the XTT assay, which measures the ability of metabolically active

236 cells to reduce tetrazolium salt. From 270 min onwards, cells exposed to rNalP exhibited a

237 statistically significant increase in absorbance compared to untreated cells (Fig. 4). In

238 contrast, at no time point did HBMECs exposed to rNalP^{S426A} or rTF show significantly

239 different absorbance to untreated cells. As expected, cells exposed to the known apoptosis-

240 inducing agent staurosporine, which would be expected to reduce cellular metabolic activity,

241 had a significantly reduced absorbance evident from 120 min post-exposure. These data show

242 that rNalP can induce an increase in HBMEC metabolic activity and this effect is mediated

243 via the proteolytic activity of rNalP.

244   We previously showed that the meningococcal autotransporter proteins App and

245 MspA are capable of clipping the histone H3 [18]. To investigate potential cellular targets for

246 rNalP proteolytic activity, we examined the ability of rNalP and rNalP^{S426A} to cleave human

247 histones (H2A, H2B, H3.1 and H4) but the absence of rNalP-specific cleavage products

248 confirmed a lack of histone clipping activity (Fig. S4).

249

250 **4. Discussion**

251   NalP is an autotransporter protease which cleaves itself, and several other

252 meningococcal proteins, on the outer surface of the bacterium [7, 10-14]. Additionally, NalP

253 cleaves human C3, which contributes to meningococcal survival in human serum [17]. Here

254 we provide evidence that NalP is internalized by human cells and induces alterations in host

255 cell biology. This is reminiscent of findings from previous studies on the IgA1P, App and

256 MspA meningococcal serine protease autotransporters [18, 20, 21]. Following cellular uptake

257 and trafficking, IgA1P cleaves the p65/RelA component of NF-kB in the nucleus, thus

258 silencing the expression of several NF-kB-responsive genes, ultimately leading to sustained

259 activation of c-Jun N-terminal kinase and apoptosis [20]. App and MspA are also internalized

260 and induce apoptosis but, in contrast to IgA1P, MspA/App-mediated apoptosis occurs via

261   cleavage of histones [18]. The receptor of IgA1P uptake is unknown, whilst uptake of App

262   and MspA requires the cooperative activity of the mannose and transferrin receptors [18].

263   The wide range of cell types able to mediate NalP internalization (including immune,

264   epithelial, endothelial and neural cells) suggests shared receptor and internalization

265   machineries, but this will require further experimentation. Additional work is also required to

266   define the region(s) of NalP which are involved, although our data shows that uptake is not

267   dependent on the proteolytic ability of NalP.

268   The contribution of NalP to pathogenesis remains incompletely understood, in part

269   because of its low abundance in culture supernatants, which has impeded the purification of

270   experimentally useful amounts of active NalP directly from meningococcal cultures.

271   Consequently, previous studies have utilized *E. coli*-derived recombinant NalP fragments

272   purified under denaturing conditions (*i.e.* non-proteolytically active) or concentrated

273   secretome preparations derived from *N. meningitidis*, which although containing active NalP,

274   lacked purity. Furthermore, wild-type and *nalP* mutant-derived secretomes are difficult to

275   compare directly given the complex alterations in secreted protein profile that are NalP-

276   expression dependent [7, 9-14, 20]. The ability of our rNalP preparation, which was purified

277   under non-denaturing conditions, to cleave human C3, confirmed the findings of Del Tordello

278   *et al.,* [17], demonstrated that the recombinant protein was catalytically active, and

279   importantly provided the opportunity to specifically address the influence of NalP and its

280   proteolytic activity in inducing changes in host cell biology. This was determined using the

281   XTT assay – an assay based on the ability of dehydrogenase enzymes produced by

282   metabolically-active cells to reduce XTT to an orange formazan dye [22]. Significant

283   alterations in the ability to reduce XTT usually result from changes in cell viability following

284   exposure to a treatment. Additional work is required to investigate if the positive effect

285   mediated by rNalP occurs in other human cell types, whether it results from increased

286 proliferation, and to define the mechanism by which the effect occurs. Our data confirm,

287 however, that the observed effect is not mediated via NalP-mediated histone clipping.

288   In summary, the use of proteolytically-active recombinant NalP has generated new

289 insights into the multifaceted role of NalP in the complex interaction between the

290 meningococcus and its obligate host by revealing that NalP is internalized by host cells and

291 that NalP proteolytic activity results in an increase in cell metabolic activity.

292

300

301 **Conflicts of interest**

302 The authors declare that there are no conflicts of interest.

303   **References**

304   1.   **Stephens DS**. Biology and pathogenesis of the evolutionarily successful, obligate

305   human bacterium *Neisseria meningitidis*. *Vaccine* 2009;27(Suppl 2):B71-77.

306   2.   **Virji M**. Pathogenic neisseriae: surface modulation, pathogenesis and infection control.

307   *Nature* 2009;7:274-286.

308   3.   **Henderson IR, Navarro-Garcia F, Desvaux M, Fernandez RC, Ala'Aldeen DAA**.

309   Type V protein secretion pathway: the autotransporter story. *Microbiol Mol Biol Rev*

310   2004;68(4):692-744.

311   4.   **Leyton DL, Rossiter AE, Henderson IR**. From self sufficiency to dependence:

312   mechanisms and factors important for autotransporter biogenesis. *Nat Rev Microbiol*

313   2012;10:213-225.

314   5.   **Benz I, Schmidt MA**. Structures and functions of autotransporter proteins in microbial

315   pathogens. *Int J Med Microbiol* 2011;301(6):461-468.

316   6.   **Turner DPJ, Wooldridge KG, Ala'Aldeen DAA**. Autotransported serine protease A

317   of *Neisseria meningitidis*: an immunogenic, surface-exposed outer membrane, and secreted

318   protein. *Infect Immun* 2002;70(8):4447-4461.

319   7.   **van Ulsen P, van Alphen L, ten Hove J, Fransen F, van der Ley P *et al.*** A Neisserial

320   autotransporter NalP modulating the processing of other autotransporters. *Mol Microbiol*

321   2003;50(3):1017-1030.

322   8.   **Oldfield NJ, Matar S, Bidmos FA, Alamro M, Neal KR *et al.*** Prevalence and phase

323   variable expression status of two autotransporters, NalP and MspA, in carriage and disease

324   isolates of *Neisseria meningitidis*. *PLoS One* 2013;8(7):e69746.

325   9.   **Roussel-Jazédé V, Grijpstra J, van Dam V, Tommassen J, van Ulsen P**. Lipidation

326   of the autotransporter NalP of *Neisseria meningitidis* is required for its function in the release

327   of cell-surface-exposed proteins. *Microbiology* 2013;159(Pt 2):286-295.

328   10.   **Serruto D, Adu-Bobie J, Scarselli M, Veggi D, Pizza M** *et al.* *Neisseria meningitidis*

329 App, a new adhesin with autocatalytic serine protease activity. *Mol Microbiol* 2003;48(2):323-

330 334.

331   11.   **Roussel-Jazédé V, Jongerius I, Bos MP, Tommassen J, van Ulsen P**. NalP-mediated

332 proteolytic release of lactoferrin-binding protein B from the meningococcal cell surface. *Infect*

333 *Immun* 2010;78(7):3083-3089.

334   12.   **Serruto D, Spadafina T, Ciucchi L, Lewis LA, Ram S** *et al.* *Neisseria meningitidis*

335 GNA2132, a heparin-binding protein that induces protective immunity in humans. *PNAS*

336 2010;107(8):3770-3775.

337   13.   **van Ulsen P, Adler B, Fassler P, Gilbert M, van Schilfgaarde M** *et al.* A novel phase-

338 variable autotransporter serine protease, AusI, of *Neisseria meningitidis*. *Microbes Infect*

339 2006;8(8):2088-2097.

340   14.   **Turner DPJ, Marietou AG, Johnston L, Ho KK, Rogers AJ** *et al.* Characterization

341 of MspA, an immunogenic autotransporter protein that mediates adhesion to epithelial and

342 endothelial cells in *Neisseria meningitidis*. *Infect Immun* 2006;74(5):2957-2964.

343   15.   **Arenas J, Nijland R, Rodriguez F, Bosma T, Tommassen J**. Involvement of three

344 meningococcal surface-exposed proteins, the heparin-binding protein NhbA, the α-peptide of

345 IgA protease, and the autotransporter protease NalP, in initiation of biofilm formation. *Mol*

346 *Microbiol* 2013;87:254-268.

347   16.   **Casellato A, Rossi Paccani S, Barrile R, Bossi F, Ciucchi L** *et al.* The C2 fragment

348 from *Neisseria meningitidis* antigen NHBA increases endothelial permeability by destabilizing

349 adherens junctions. *Cell Microbiol* 2014;16(6):925-937.

350   17.   **Del Tordello E, Vacca I, Ram S, Rappuoli R, Serruto D**. *Neisseria meningitidis* NalP

351 cleaves human complement C3, facilitating degradation of C3b and survival in human serum.

352 *PNAS* 2014;111(1):427-432.

353   18.   **Khairalla AS, Omer SA, Mahdavi J, Aslam A, Dufailu OA *et al.*** Nuclear trafficking,

354   histone cleavage and induction of apoptosis by the meningococcal App and MspA

355   autotransporters. *Cell Microbiol* 2015;17(7):1008-1020.

356   19.   **Lin L, Ayala P, Larson J, Mulks M, Fukuda M *et al.*** The Neisseria type 2 IgA1

357   protease cleaves LAMP1 and promotes survival of bacteria within epithelial cells. *Mol*

358   *Microbiol* 1997;24(5):1083-1094.

359   20.   **Besbes A, Le Goff S, Antunes A, Terrade A, Hong E *et al.*** Hyperinvasive

360   meningococci induce intra-nuclear cleavage of the NF-kappaB protein p65/RelA by

361   meningococcal IgA protease. *PLoS Pathog* 2015;11(8):e1005078.

362   21.   **Pohlner J, Langenberg U, Wölk U, Beck SC, Meyer TF**. Uptake and nuclear

363   transport of Neisseria IgA1 protease-associated α-proteins in human cells. *Mol Microbiol*

364   1995;17(6):1073-1083.

365   22.   **Scudiero DA, Shoemaker RH, Paull KD, Monks A, Tierney S *et al.*** Evaluation of a

366   soluble tetrazolium/formazan assay for cell growth and drug sensitivity in culture using human

367   and other tumor cell lines. *Cancer Res* 1988;48(17):4827-4833.

368
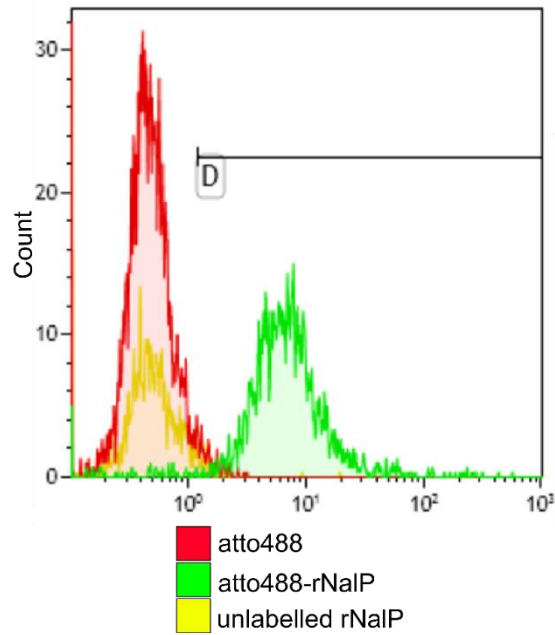
Fig. 1. Flow cytometric analysis showing the binding of rNalP to human brain microvascular endothelial cells (HBMECs). HBMECs treated with atto488 alone (red) were compared with HBMECs treated with atto488-rNalP (green) and unlabeled rNalP (yellow). Data was acquired on a Beckman Coulter FC500 flow cytometer and is displayed as a histogram. The histogram area in D represents the population of fluorescently labelled HBMECs.

375
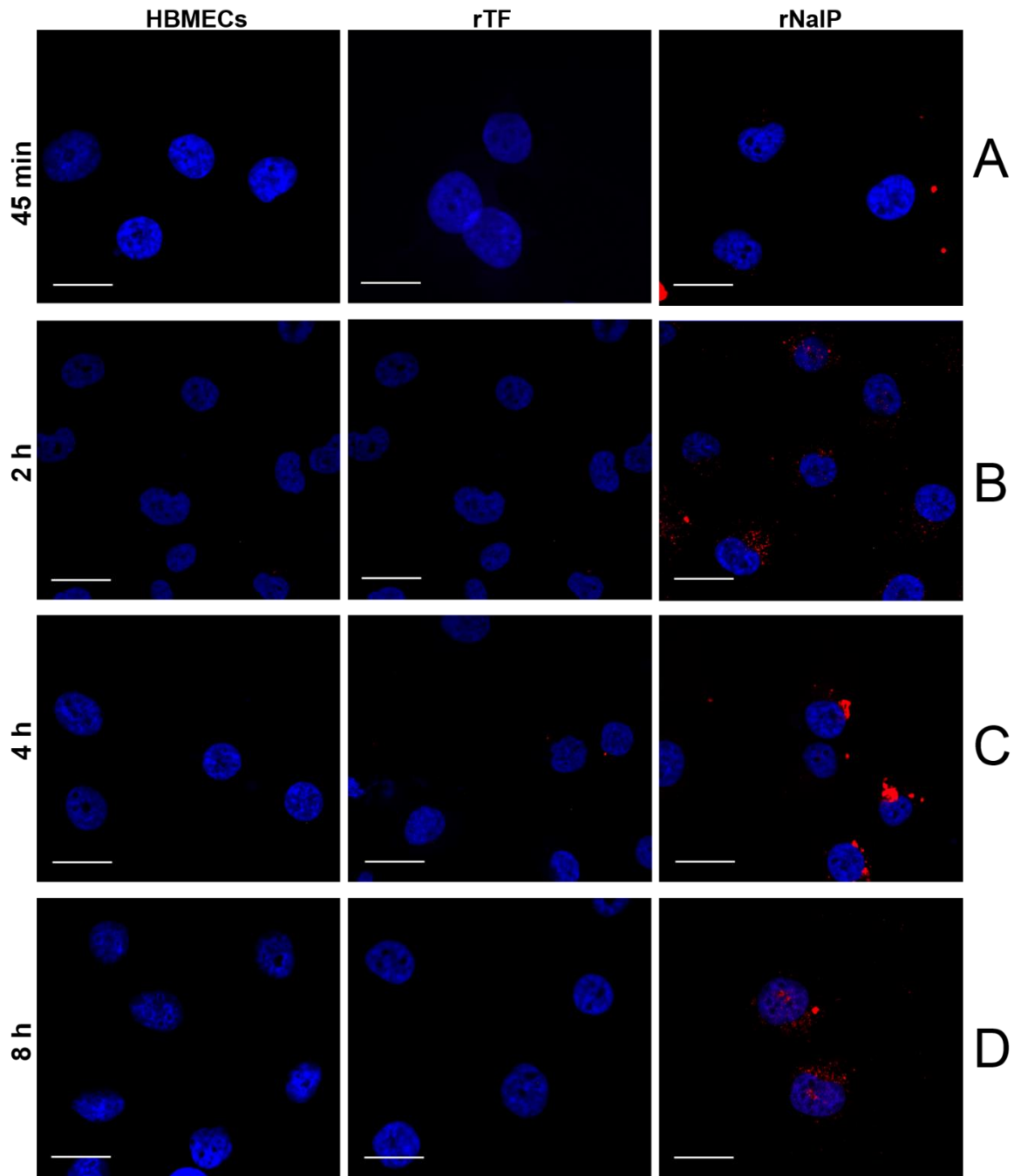
Fig. 2. Cellular uptake of rNalP into human brain microvascular endothelial cells

(HBMECs). HBMECs were left untreated or co-incubated with Cy5-labelled rTF or rNalP

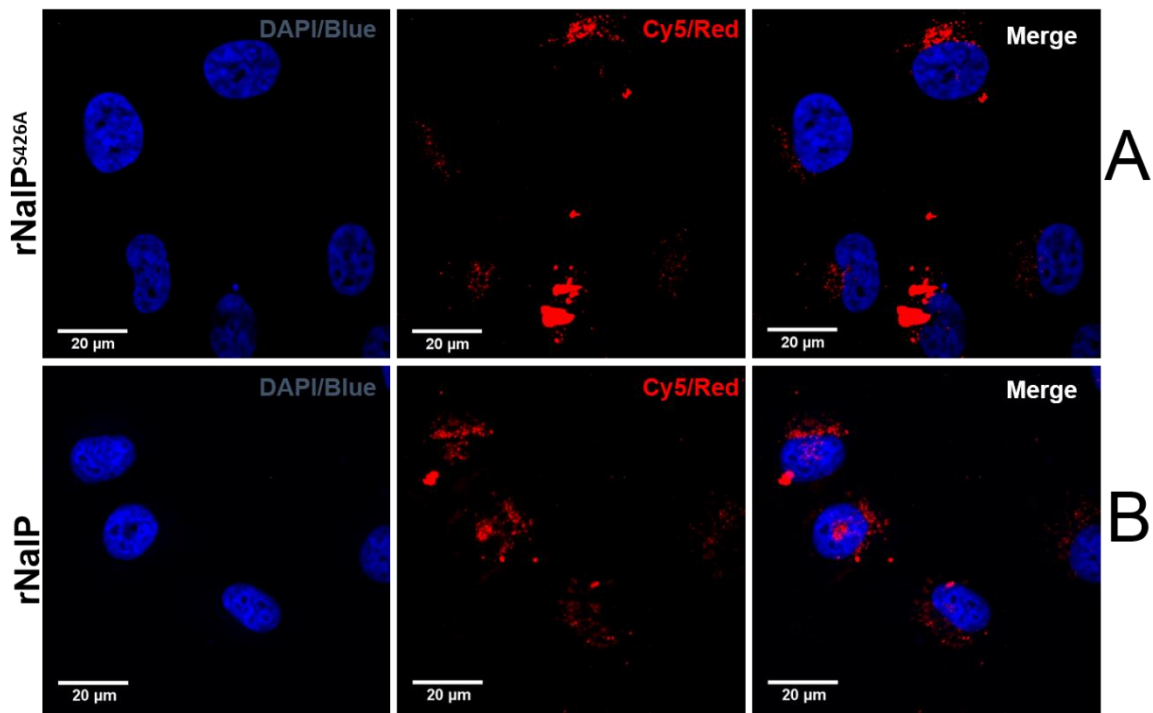for 45 min (A), 2 h (B), 4 h (C) or 8 h (D). Cell nuclei were stained with DAPI. Cells were

washed and fixed before analysis by confocal laser microscopy. All images were scanned at a

resolution of 1024×1024 pixels, using the same laser and gains settings. The cells are

representative of cells observed from three independent experiments. Scale bars = 20 µm.

382

383

Fig. 3. rNalP proteolytic activity is not required for cellular uptake and perinuclear localization by HBMECs. HBMECs were treated with Cy5-labelled rNalP^{S426A} (A) or rNalP (B) for 8 h. Cell nuclei were stained with DAPI, washed and fixed before scanning using confocal laser microscope. All images were scanned at a resolution of 1024×1024 pixels, using the same laser and gains settings. The cells are representative of cells observed from multiple experiments. Scale bars $= 20\ \mu$m.
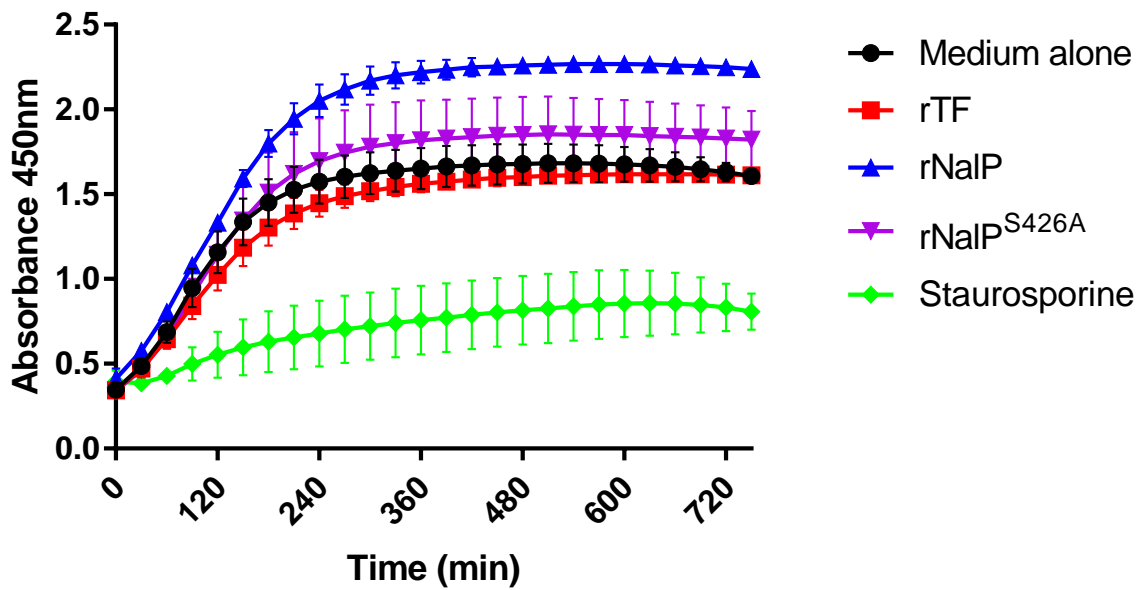
Fig. 4. Exposure of HBMECs to rNalP induces an increase in cell metabolic activity.

HBMECs were treated with medium alone, rTF, rNalP, rNalP^{S426A} or staurosporine in triplicate. Cell metabolic activity was assessed using the XTT assay kit via absorbance readings at 450 nm over 750 min. Values shown are the mean ± SE from three independent experiments and were analyzed by two-way ANOVA and Tukey's multiple comparison test. Significant increases in absorbance were induced by rNalP ($p < 0.05$ from 270 min; $p < 0.005$ from 600 min). rNalP^{S426A} and rTF induced no significant difference compared to media alone at any time point, whilst staurosporine induced a significant reduction in absorbance compared to treatment with media alone ($p < 0.01$ from 120 min; $p < 0.001$ from 150 min; $p < 0.0001$ from 180 min).